Proceedings of the 21st ICSMGE, Vienna, Austria, 14 – 19 June 2026. Pistrol, Adam & Schweiger (eds.)
Published by: ÖGG, Austrian Society for Geomechanics, Salzburg, Austria, ISBN 978-3-9503898-4-5
https://doi.org/10.53243/ICSMGE2026-2223

Numerical investigation of the role of artesian pressure on the initiation of sensitive clay landslide

Shishir Amit, Bipul Hawlader
Memorial University of Newfoundland, St. John's, NL, Canada, sksamit@mun.ca

Ripon Karmaker
Stantec Consulting Ltd., St. John's, NL, Canada

Rajib Dey
WSP, Mississauga, Ontario, Canada

ABSTRACT: Artesian water pressure can be developed from groundwater flow through a highly permeable layer below the lower permeable sensitive clay layer. The effects of artesian pressure on slope failure are investigated in this study. The commercially available software packages, namely SEEP/W, SLOPE/W and SIGMA/W, are used to calculate the stresses in soil and factor of safety. Analyses are performed by placing a highly permeable soil layer at various depths below the toe with varying thicknesses and hydraulic conductivities. The increase in hydraulic conductivity of the highly permeable layer reduces the factor of safety (*Fs*) if it is closer to the bottom of the river, and the *Fs* reduces more quickly with an increase in thickness of the highly permeable layer. Negligible effects on slope stability are found when the highly permeable layer is sufficiently far from the riverbed. The soil is more localized around the toe when the artesian pressure is developed; however, such failure of a small soil block could trigger upward progressive failure and cause a large landslide.

KEYWORDS: Artesian pressure, groundwater flow, sensitive clay, limit equilibrium analysis.

1 INTRODUCTION

Many small to large-scale landslides occur in Canadian and Scandinavian sensitive clays. For example, on average, 1–2 large landslides occur annually in Canada and Norway that involve more than 50,000 m^3 of soil (Demers et al. 2014; L'Heureux et al. 2018; Søvik et al. 2025). Large landslides generally occur through progressive failure of a number of soil blocks within a few minutes. In an upward progressive failure, the failure can be triggered only if a soil block fails near the toe. Therefore, the stability of the first soil block is the main concern.

Previous studies discussed the effects of drainage on stability analysis. For example, Lefebvre (2017) presented a discussion on drained versus undrained analyses to assess the stability of the first soil block. Drained analysis was recommended considering the valley formation process in Eastern Canadian sensitive clays. Drained analysis has also been conducted in previous studies. For example, Lo and Lee (1974) and Lefebvre (1981) conducted back analyses of several slope failure cases in Canada using limit equilibrium (LE) methods for drained conditions. The drained soil parameters (i.e., cohesion (c') and angle of internal friction (ϕ')) were obtained from triaxial tests under lower confining pressure as encountered below the slope where the failure plane forms. Drained triaxial test results show strain-softening behaviour after the peak. Such strain softening could result in progressive formation of the failure plane, as described by Leroueil et al. (2012) based on several case studies. Progress failure and strain softening cannot be explicitly modelled in the LE methods. Therefore, previous studies suggested using the post-peak shear strength parameters derived from mobilized strength in the drained triaxial tests at ~8% of axial strain (Lefebvre 1981).

Once the failure is triggered, the landslide might occur within a few minutes. Therefore, the retrogression process can be modelled in undrained conditions. Several numerical techniques have been developed to model the large deformation in sensitive clay landslides (e.g., Dey et al. 2015; Wang et al. 2022; Zhang et al. 2019). Some of these studies triggered the failure by toe erosion, which is one of the main causes of landslides in sensitive clays (L'Heureux et al. 2014; Thakur et al. 2017). The size and shape of the erosion block (i.e., small soil block that fails near the toe) need to be defined in these numerical studies. In addition to the other factors (e.g., slope geometry, soil type), the groundwater conditions, especially the artesian pressure, could be one of the main causes of failure of a soil block near the toe. For example, artesian pressure was one of the main factors that triggered the Saint-Jude landslide in Quebec, Canada (Locat et al. 2017).

Lefebvre (2017) explained the effects of groundwater flow on sensitive clay landslides in Eastern Canada. It has been reported that a highly permeable soil layer can exist below the sensitive clay and above the bedrock. If the riverbed is far from or at the highly permeable layer, the groundwater flow through the highly permeable layer would not reduce the stability of the slope. However, if it is in between, artesian pressure can significantly reduce the effective stress in the soil below the toe, which could initiate the failure.

The objective of this study is to examine the effects of a highly permeable layer on the stability of the slope. Seepage, stress deformation and limit equilibrium analyses are performed to calculate the stresses in soil and the factor of safety.

2 PROBLEM STATEMENT

Figure 1(a) shows the process of valley formation in sensitive clays in Eastern Canada, as described by Lefebvre (2017). Generally, in this area, the sensitive clay unit of lower hydraulic conductivity is sandwiched between two soil layers of higher hydraulic conductivity, namely the upper crust and a soil layer immediately above the bedrock (typically till), which is called 'high permeable layer' in this study. The hydraulic conductivity of the high permeable layer (k_{hp}) could be more than 100 times that of the sensitive clay layer (k_{s}). Depending upon the depth of the high permeable layer, there could be a thick sensitive clay layer below the riverbed (stage I in Fig. 1(a) while, in some cases, the riverbed might reach the high permeable layer (stage III in Fig. 1(a)). In other words, the depth of the high permeable layer below the riverbed (h_{p}) varies. Also, the thickness of the high permeable layer (t_{p}) might vary. Now, depending upon h_{p},

t_p and k_{hp}/k_s, an artesian pressure can generate in the soil elements near the toe, which can increase the failure potential of a soil block near the toe and progressive failure in a large landslide.

The GeoStudio 2D software is commonly used in the industry, which has the advantage of combining multiple analyses for a single project. In the present study, SEEP/W, SLOPE/W and SIGMA/W are used to model seepage, evaluate the factor of safety, and calculate the stress state, respectively, for the slope.

Figure 1(b) shows the geometry of the slope considered in this study, which is similar to a typical sensitive clay slope near the riverbank in Quebec, Canada. A 20-m high 2.5H:1V slope is analyzed. The slope consists of a 2-m thick clay crust below the ground surface and slope, more than 20-m thick sensitive clay layer, a higher permeable soil layer of thickness t_p at a depth of h_p below the toe, and a bottom soil layer. The thickness, depth and hydraulic conductivity of the higher permeable layer are varied to check their effects on the stability of the slope. The hydraulic conductivities of the crust and bottom layers are k_c and k_b, respectively. To minimize boundary effects on the results, the left and right boundaries are placed at 100 m and 290 m from the toe and crest, respectively. It is to be noted here that the riverbed width could be smaller than this, and, in that case, the opposite riverbank can affect the results; however, this has not been investigated in the present study. The bottom boundary is 40 m below the toe.

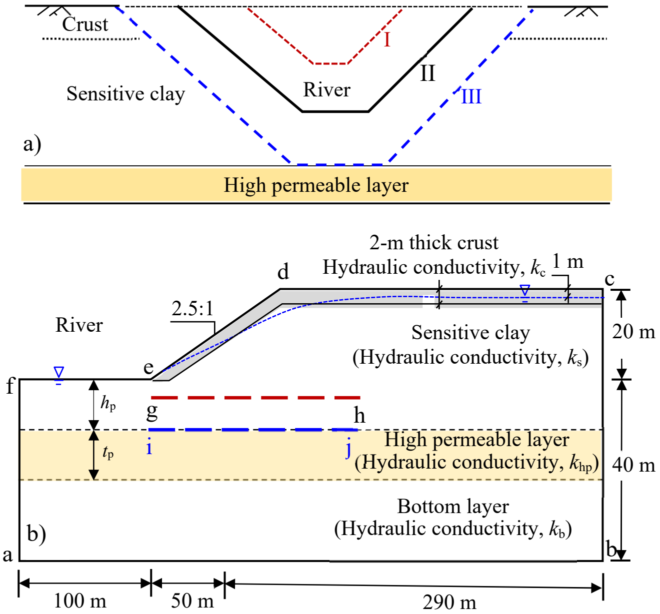

Figure 1. Problem statement: a) three stages of valley formation (based on Lefebvre 2017); (b) Model geometry.

Water elevation in the river is assumed to be at the level of the toe. The groundwater level is assumed to be at 1 m below the ground surface from 30 m from the crest. The left, right and bottom boundaries are impermeable, while free seepage conditions are applied to the slope surface. The seepage analysis provides the phreatic surface at the steady state conditions, as shown schematically by the blue dotted line in Fig. 1. The location of the phreatic surface depends on the hydraulic conductivity of the soil layer, as discussed in the following sections, which affects the factor of safety of the slope.

The analyses started with the modelling of seepage using SEEP/W. The seepage analysis is performed for the steady-state conditions, and the results (e.g., pore pressure distribution) are transferred to SLOPE/W to calculate the factor of safety and the location of the critical circle. Finally, SEEP/W results are used in SIGMA/W to calculate stresses in the soil.

3 GEOTECHNICAL PROPERTIES

Table 1 shows the geotechnical parameters used in the analysis. The value of hydraulic conductivity is selected based on previous studies in which the hydrogeological conditions of the landslide-prone areas of Canadian sensitive clays have been investigated (Lefebvre 2017; Locat et al. 2017; Tremblay-Auger 2021).

The Mohr–Coulomb model is used to define the shear strength of soil. Lo and Morin (1972) and Lefebvre (1981) conducted triaxial tests on sensitive clays after consolidating the specimens from low pressures as encountered below the slope to high values of up to 400 kPa. They observed post-peak softening in stress–strain behaviour. It has been suggested to use the post-peak shear strength, as mentioned in the introduction, in limit equilibrium analysis to assess the stability of the first soil block. They also found a nonlinear strength envelope for the post-peak conditions. However, for simplicity, a constant value of ϕ' (= 32°) is used for the sensitive clay layer, which is similar to the value used in previous studies (e.g., Locat et al. 2017). Laboratory tests also show that, unlike ϕ', cohesion intercept (c') is almost independent of confining pressure (Lefebvre, 1981). Based on these studies, $c' = 6$ kPa is used for sensitive clay. Lo and Morin (1972) also calculated Young's moduli for varying confining pressures. Based on that study, a Young's modulus of 15 MPa is used for sensitive clay. A higher friction angle of 40° is used for the high permeable soil layer. The bottom layer below the high permeable layer is modelled as a very low-permeable and high-strength material (e.g., bedrock). The failure plane does not reach this layer, and no significant seepage occurs in this layer. However, this layer is added to avoid boundary effects on calculated results.

Table 1. Geotechnical properties used for analysis.

Parameter	Crust	Sensitive clay	High permeable layer	Bottom layer
Saturated unit weight, γ_{sat} (kN/m^3)	17	17	17	17
Hydraulic conductivity, k (m/s)	10^{-7}	10^{-9}	10^{-8}–10^{-6}	9×10^{-12}
Cohesion, c' (kPa)	6	6	5	5
Angle of internal friction, ϕ' (°)	30	32	40	45
*Young's modulus, E (MPa)	15	15	30	35
*Poisson's ratio, ν'	0.33	0.33	0.33	0.33

*Parameters used for SIGMA/W analysis

4 RESULTS

Figure 2 shows the effects of the high permeable layer on the factor of safety. The analyses are performed placing the high permeable layer at 4 m (solid lines) and 10 m (dashed lines) depths below the riverbed and for varying hydraulic conductivity of the high permeable layer (k_{hp} = 10^{-8}–10^{-6} m/s, i.e., k_{hp}/ k_s equal to 1 (uniform soil) to 1,000) and thickness (t_p = 2 m – 10 m). When the high permeable layer is at 4 m depth, the *Fs* gradually decreases with an increase in hydraulic conductivity of the high permeable layer. For example, the failure of a soil block is possible (i.e., Fs < 1.0) when a 6-m thick high permeable soil layer exists at a depth of 4 m below the toe and has a hydraulic conductivity 550 times higher than that of the sensitive clay layer. For the same depth (h_p = 4 m), the rate of decrease of the factor of safety is higher for a thicker high permeable layer. There is a slight increase in *Fs* at low k_{hp}/k_s, which is due to the change in flow direction that lowers the phreatic line.

When the high permeable layer is at 10 m depth below the toe, the *Fs* does not decrease with an increase in hydraulic conductivity of the high permeable layer (dashed lines in Fig. 2). Instead, there is a slight increase in *Fs* with an increase in hydraulic conductivity of the high permeable layer. Again, such an increase in *Fs* is due to the change in flow direction and phreatic line.

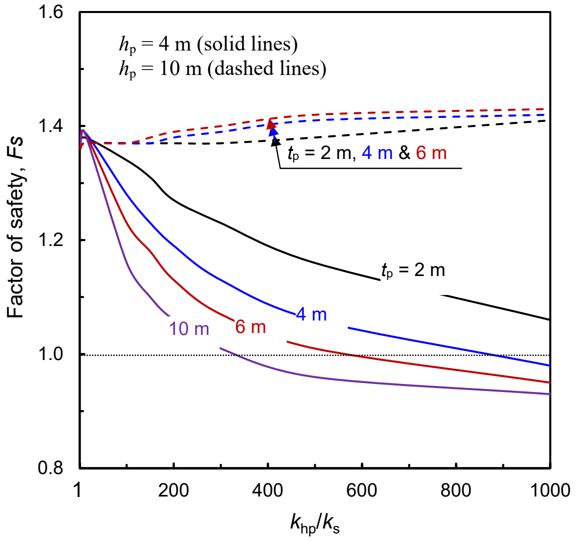

Figure 2. Effects of high permeable soil layer on factor of safety.

The effects of high permeable layer can be better understood from the stresses in soil elements near the toe, where high artesian pressure develops. The soil elements along two lines are considered for this purpose: (i) at the boundary between the sensitive clay layer and high permeable layer (line *ij* in Fig. 1(b)), where high artesian pressure develops, and (ii) at 2 m below the toe (line *gh* in Fig. 1(b)).

The solid lines in Fig. 3 show the pore pressure in the soil elements at 4 m depth (along line *ij*) with distance from the toe (toe position is at 100 m in the horizontal axis). The pore pressure gradually increases with horizontal distance. When compared the results for different hydraulic conductivities, the pore pressure goes up in the soil elements along the line *ij*, approximately up to the middle of the slope, with an increase in hydraulic conductivity of the high permeable layer. For example, the pore pressure is increased approximately 30 kPa in the soil element at 4 m depth under the toe for an increase in k_{hp}/k_s from 1 to 200. A similar trend is found for the soil elements at 2 m depth below the toe (i.e., along line *gh* in Fig. 1(b)), as shown by the two dashed lines for k_{hp}/k_s = 1 and 500. Such an increase in artesian pressure reduces the effective stress and could cause the failure of the slope. Approximately from the mid-slope position (x > 120 m), the pore pressure decreases with an increase in k_{hp}/k_s. Figure 3 also shows the total vertical stress in these soil elements for k_{hp}/k_s = 1. No significant change in total stress with an increase in k_{hp}/k_s is found. Therefore, the reduction of vertical effective stress occurs mainly up to the midslope position for the cases analyzed. In other words, this is the critical zone from where failure might be initiated due to artesian pressure, if the other conditions remain the same.

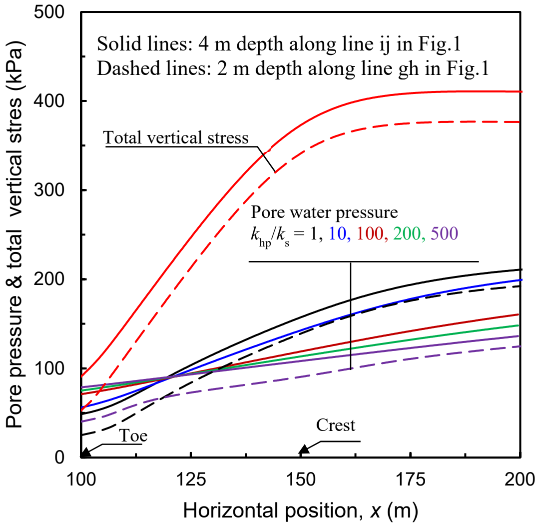

Figure 3. Effects of high permeable soil layer on factor of safety.

Figure 4 shows the location of the critical circle and phreatic surface when a 4-m thick high permeable layer exists 4 m below the riverbed for varying k_{hp}/k_s (= 1–500). The dashed lines in Fig. 4 show the location of the phreatic line near the slope that influences the stability of the slope. The phreatic level drops with an increase in hydraulic conductivity of the high permeable layer, especially under the crest of the slope. However, the difference between the phreatic levels is not significant for higher k_{hp}/k_s values (> 100). Nevertheless, the phreatic line from the toe to mid-slope remains almost the same for varying k_{hp}/k_s.

The critical circle for all the cases starts from a point approximately 10 m left of the toe. On the right side, the critical circle intersects the slope or ground surface at different distances depending upon the ratio of k_{hp}/k_s. The largest soil block above the critical circle is obtained for the same hydraulic conductivity (k_{hp}/k_s =1). Note that, among these critical circles, the last two for k_{hp}/k_s = 500–1000 represent the potential failure conditions (Fs ~ 1.0) (see Fig. 2). While the soil above these critical failure planes (thick lines) is relatively small, it has significant practical implications. The failure of this small block might trigger a retrogressive landslide in sensitive clay. Also, this block might provide an idea for estimating the size and shape of the soil block for undrained modelling of large-scale landslides in sensitive clay.

5 CONCLUSIONS

This study presents the influence of artesian pressure near the toe of a slope that could be developed due to the presence of a highly permeable soil layer below the slope. A higher contrast in hydraulic conductivities between the sensitive clay layer and the highly permeable layer increases the artesian pressure, primarily near the toe. Artesian pressure development and failure potential increase when the riverbed moves closer to the highly permeable layer. The proposed approach could be used to assess the stability of a riverbank if the riverbed continues to move towards the highly permeable layer due to erosion. The geometry of the failed soil block could be used to define the erosion block to trigger landslides in numerical simulations.

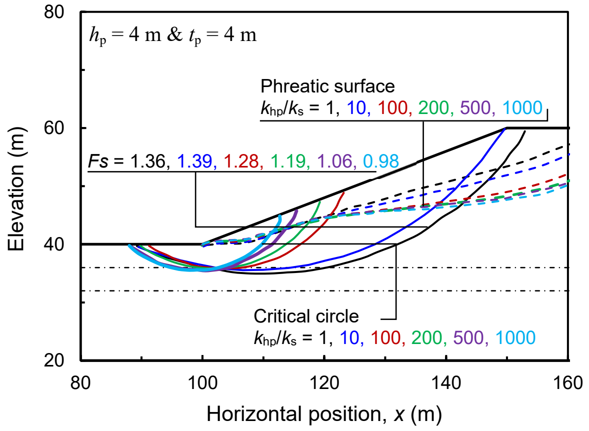

Figure 4. Effects of high permeable soil layer on factor of safety.

One of the limitations of this study is that the failure of the soil block is assessed using the limit equilibrium method, which cannot model the progressive formation of the failure plane. Also, the failure plane is assumed to be circular, which might be different, especially when the artesian pressure is developed. These issues could be examined with stress–deformation analysis using advanced finite element modelling techniques by implementing an appropriate soil model for strain softening.

6 ACKNOWLEDGEMENTS

The works presented in this paper have been supported by the Natural Sciences and Engineering Research Council of Canada (NSERC), WSP and Mitacs.

7 REFERENCES

Demers, D., Robitaille, D., Locat, P. and Potvin, J., 2014. Inventory of Large Landslides in Sensitive Clay in the Province of Québec, Canada: Preliminary Analysis. In: J.-S. L'Heureux, A. Locat, S. Leroueil, D. Demers and J. Locat. (eds.). Landslides in Sensitive Clays, Advances in Natural and Technological Hazards Research. Dordrecht: Springer Netherlands. pp.77–89.

Dey, R., Hawlader, B., Phillips, R. and Soga, K., 2015. Large deformation finite-element modelling of progressive failure leading to spread in sensitive clay slopes. Géotechnique, 65(8), 657–668.

Lefebvre, G., 1981. Fourth Canadian Geotechnical Colloquium: Strength and slope stability in Canadian soft clay deposits. Canadian Geotechnical Journal, 18(3), 420–442.

Lefebvre, G., 2017. Sensitive Clays of Eastern Canada: From Geology to Slope Stability. In: V. Thakur, J.-S. L'Heureux and A. Locat, eds. Landslides in Sensitive Clays, Advances in Natural and Technological Hazards Research. Cham: Springer International Publishing. pp.15–34.

Leroueil, S., Locat, A., Eberhardt, E., and Kovacevic, N. 2012. Keynote Lecture: Progressive failure in natural and engineering slopes. In Proc. 11th International and 2nd North American Symposium on Landslides, 3–8 June, Banff, Alta. pp. 31–46.

L'Heureux, J. S., Locat, A., Leroueil, S., Demers, D., and Locat, J., 2014. Landslides in sensitive clays: from geosciences to risk management. Advances in natural and technological hazards research 36. Springer, Dordrecht.

L'Heureux, J.S., Høydal, Ø.A., Paniagua Lopez, A.P. and Lacasse, S., 2018. Impact of climate change and human activity on quick clay landslide occurrence in Norway. In: 2nd JTC1 Workshop on Triggering and Propagation of Rapid Flow-like Landslides. Hong Kong, 5–7.

Locat, A., Locat, P., Demers, D., Leroueil, S., Robitaille, D. and Lefebvre, G., 2017. The Saint-Jude landslide of 10 May 2010, Quebec, Canada: Investigation and characterization of the landslide and its failure mechanism. Canadian Geotechnical Journal, 54(10), 1357–1374.

Lo, K.Y. and Lee, C.F., 1974. An evaluation of the stability of natural slopes in plastic Champlain clays. Canadian Geotechnical Journal, 11(1), 165–181.

Lo, K.Y. and Morin, J.P., 1972. Strength anisotropy and time effects of two sensitive clays. Canadian Geotechnical Journal, 9(3), 261–277.

Søvik, M.M., L'Heureux J-S, Rødvand, L, and Grimstad, G., 2025. A novel framework for predicting landslide mechanism in Norwegian quick clays. IOP Conf. Series: Earth and Environmental Science 1523 (2025) 012013.

Thakur, V., L'Heureux, J.S., Locat, A., 2017. Landslide in sensitive clays – from research to implementation. Advances in Natural and Technological Hazards Research, V. Thakur, J-S L'Heureux and A. Locat ed., Springer: pp. 1–11.

Tremblay-Auger, F., Locat, A., Leroueil, S., Locat, P., Demers, D., Therrien, J. and Mompin, R., 2021. The 2016 landslide at Saint-Luc-de-Vincennes, Quebec: geotechnical and morphological analysis of a combined flowslide and spread. Canadian Geotechnical Journal, 58(2), 295–304.

Wang, C., Hawlader, B., Perret, D., and Soga, K., 2022. Effects of geometry and soil properties on type and retrogression of landslides in sensitive clays. Géotechnique, 72(4), 322–336.

Zhang, W., Randolph, M.F., Puzrin, A.M. and Wang, D., 2019. Transition from shear band propagation to global slab failure in submarine landslides, Canadian Geotechnical Journal, 56(4), 554–569.